Collision Resilient V2X Communication via Grant-Free NOMA

Bashar Tahir[†], Stefan Schwarz[†], and Markus Rupp

Institute of Telecommunications, Technische Universität (TU) Wien, Vienna, Austria

Abstract—In vehicle-to-everything (V2X) communication, vehicles will perform the resources selection on their own, once there is no central coordination of the transmissions by the base station. If the vehicles choose to contest the same time-frequency resources, then a collision of the transmitted messages will occur. This can highly impact the reliability and latency of the vehicular link, which are crucial for safety-related applications. In this paper, we propose applying the framework of grant-free non-orthogonal multiple access (NOMA) for a collision resilient V2X communication. Grant-free NOMA allows for uncoordinated transmissions and can resolve collisions by means of specially designed transmit signatures, combined with an advanced receiver that utilizes the structure of those signatures. Our initial results suggest that such a framework has the potential to substantially enhance the system robustness to collisions, in terms of both reliability and latency.

I. INTRODUCTION

Future vehicles will be able to communicate wirelessly with their surrounding environment through the technology of vehicle-to-everything (V2X) [1]. Whether it is the communication with neighboring vehicles, known as vehicle-to-vehicle (V2V), with the infrastructure on the roads, i.e., vehicle-to-infrastructure (V2I), with pedestrians crossing the street, i.e., vehicle-to-pedestrian (V2P), etc. Such a connectivity will greatly enhance road safety, improve traffic management (by better routing of the vehicles), and provide broadband services on the go [2]. Those different services have varying quality-of-service requirements; especially for road safety, safety-critical messages carrying position, velocity, trajectory, etc, should be delivered with high reliability and in a timely manner [3].

Currently, there are two major standards targeting V2X [4]: dedicated short-range communication (DSRC) which is based on the IEEE 802.11p standard and its evolution 802.11bd, and the 3GPP cellular-V2X (C-V2X) building on long-term evolution (LTE) and 5th generation new-radio (5G-NR). On top of the differences between the two standards in terms of the physical (PHY) and medium access control (MAC) layers, C-V2X can utilize the cellular infrastructure to further improve the connectivity between the vehicles over long ranges, as well as perform centralized scheduling of the resources [4]; however, an out-of-coverage mode is also defined for C-V2X when the vehicles cannot be served by the cellular base station (BS). In that case, the vehicles will perform the resources

selection on their own in a local manner (similar to DSRC); hence it may occur that multiple vehicles contest the same time-frequency resources, causing collisions of the transmitted messages. In order to tackle this issue, both standards have collision avoidance mechanisms that can reduce the collision probability. In DSRC, this is achieved by carrier sense multiple access (CSMA), while in C-V2X, sensing-based semi-persistent scheduling (SB-SPS) is employed [5]. Nevertheless, collisions can still occur. For example, in the case of high vehicle density, the resources will be heavily contested [6], and after a certain amount of time, the vehicles will have to transmit their messages anyway due to the strict latency budget of the safety-related applications. Also, if multiple vehicles start sensing at the same time, then they might end up selecting the same resources. This is further complicated by the time-varying nature of the process; vehicles join and leave a certain communication range all the time.

In order to enhance the robustness to collisions in terms of reliability and latency, we propose applying the framework of grant-free non-orthogonal multiple access (NOMA) for a collision resilient V2X communication. Grant-free NOMA is currently under investigation for the uplink of 5G-NR with many schemes proposed [7], [8]. Those schemes have shown the ability to support massive connectivity and reduce access latency, and are especially suited for the applications of massive machine-type communication (mMTC) [9]. The motivation behind applying such a framework in the context of V2X is twofold: first, if the system is expected to have collisions, i.e., the devices access is non-orthogonal, then it would make sense to have a system that is designed from the ground to be non-orthogonal. This includes proper design of the transmit signal, and an advanced receiver that can resolve this non-orthogonality; second, having a system that is robust to collisions results in less dropped packets, which translates into a lower latency communication.

A power-domain NOMA scheme has been applied in [10] to enhance V2X transmission reliability and latency; however, the scheme assumes that the scheduling is carried out by the BS, and employs a distributed power control via feedback between the vehicles. The framework applied here is grant-free, and therefore the vehicles communicate directly with no scheduling/control signaling required. What we investigate here is the application of such a scheme in the case where there is no coordination by the BS, i.e., out-of-coverage. The NOMA framework in this paper is based on interleave-grid multiple access (IGMA) [11]. In the next section we explain
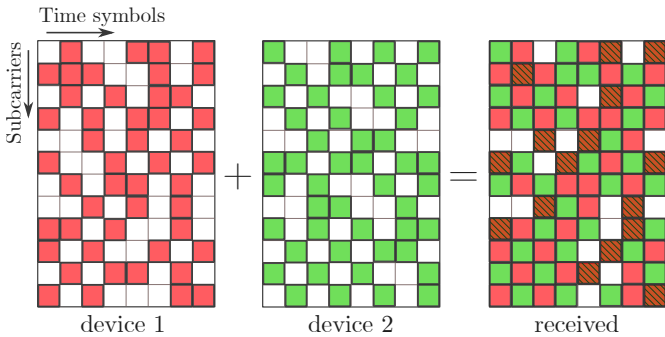
Fig. 1: Mapping of the symbols.

how it is applied, and discuss the signal design and detection. We investigate the performance of such a system from a link-level perspective in terms of the average block error ratio (BLER) and in terms of packets latency. Our initial results suggest that grant-free NOMA has the potential of improving the performance of uncoordinated V2X transmissions, even in the case where four vehicles are constantly interfering with each other.

II. GRANT-FREE NOMA

A. Scheme Description

The framework of grant-free transmission is currently being investigated for the uplink of 5G-NR using NOMA. The main idea of such schemes, is that the devices can transmit on their own without a coordination by the BS, i.e., grant-free, which helps in reducing the access latency; however, since the transmission is uncoordinated, collisions occur when two or more devices pick the same time-frequency resources. This is where the NOMA techniques come into play. The different devices transmit their messages using a signature that is picked from a predefined pool. Those signatures could be interleaving patterns at the bit-level [12], or short spreading sequences on the symbol-level that have certain properties, such as being sparse [13], or dense with low cross-correlation [14], [15], which in turn facilitates different detection algorithms. There exist also many other schemes, e.g., utilizing scrambling sequences [16], etc. The receiver, in general, has to perform user activity detection [17] (by utilizing the patterns), followed by other standard procedures, such as NOMA channel estimation, and data detection, typically in an iterative manner.

The scheme we apply here can be considered as a variant of the IGMA scheme proposed in [11], in which we do not apply any device-specific bit interleaving and we employ a low-complexity interference cancellation detector. We assume that the transmission is based on orthogonal frequency-division multiplexing (OFDM). Once each device has data to transmit, the symbols are mapped in a spread manner onto the selected time-frequency resources. This is illustrated in Figure 1. Each device randomly picks a mapping pattern from a predefined pool. The larger is the pool, the less likely that two devices pick the same pattern. Since the patterns are random, some symbols will be received interference-free, while others will

collide with the symbols of the other devices at the positions where the patterns overlap, as shown in the figure. Each pattern can be generated as a vector of 1's and 0's, where the 1's indicate the positions where the data symbols are mapped. For example, consider the following mapping patterns stacked as row-vectors in the matrix

$$\mathbf{P} = \begin{bmatrix} 0 & 1 & 1 & 1 & 0 \\ 1 & 0 & 1 & 0 & 1 \end{bmatrix} . \tag{1}$$

The pattern given by the first row maps the data symbols only to the 2nd, 3rd, and 4th positions of the time-frequency grid, while the second pattern maps the data symbols to the 1st, 3rd, and 5th positions. Therefore, the two devices picking those patterns will only interfere at the 3rd position.

Let the total number of positions in the selected time-frequency resources be N_{total}, and the number of data symbols be N_{data}, we define the expansion factor as

$$L = N_{total}/N_{data} . \tag{2}$$

For $L = 2$, it means that half the symbols are data, and the other half are not used (zeros) according to the chosen pattern. When comparing it against an orthogonal multiple access (OMA) system, an OMA device occupies the entire time-frequency block, i.e., it transmits more data symbols. Therefore, in order to have a fair comparison, the code-rate of the NOMA system is increased by the expansion factor, such that the effective rate stemming from the bit-level channel coding and the symbol-level expansion (if any), is equivalent for both OMA and NOMA. In other words, for an OMA system with code-rate R_b, the code-rate of the NOMA system is set to $R'_b = R_b \times L$. This guarantees that both systems are running with the same effective rate. The value of L has to be chosen carefully: setting L too high will risk losing the gain of channel coding. In other words, shifting the redundancy from bit- to symbol-level for the sake of better interference suppression should be treaded carefully. Obviously, it depends on how many devices are expected to interfere with each other. The attractive feature of this scheme is that L can be adjusted almost arbitrarily (e.g., $L = 1.5$); compared to the sequence-based spreading schemes, the spreading length can only be an integer, i.e., $L = 2, 3, 4$, etc. This is actually the reason why we consider the IGMA scheme here. Unfortunately, choosing L is not an easy task, and we have to rely on simulations to determine a suitable value for a given deployment scenario.

Besides the impact on the code-rate, the zero positions of the patterns carry no signal, and therefore the resultant average transmit power of the NOMA scheme over the entire time-frequency block will be less than that of OMA. To account for that, instead of scaling the data symbols by $\sqrt{P_k}$ (as in OMA), where P_k is the transmit power of the kth device; they are scaled by $\sqrt{LP_k}$. In other words, the transmit power of the data symbols at the non-zero positions of the pattern, are boosted by a factor of L. This then ensures that the average transmit power across the entire time-frequency block (including the zero positions) is identical to OMA.
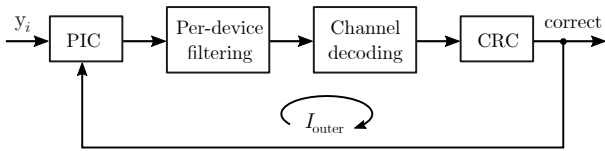
Fig. 2: Iterative CWL-PIC receiver.

B. Detection

Let K be the number of active devices. After applying the inverse fast-Fourier-transform (FFT) at the transmitters and the FFT at the receiver, the received signal at the ith position on the time-frequency grid is given by

$$y_i = \sum_{k=1}^{K} h_{k,i} x_{k,i} + n_i \ , \quad i = 1, 2, \ldots, N_{\text{total}} \ , \qquad (3)$$

where $h_{k,i}$ is the effective fading coefficient of the kth device at the ith index, which encompasses both the transmit power and channel fading, $x_{k,i}$ is the corresponding transmit signal, and n_i is the Gaussian noise. The detection is performed per-device in parallel, treating other interferers as noise, followed by parallel interference cancellation (PIC) on the codeword level (CWL), as shown in Figure 2.

The detected symbols of the kth device are given by

$$\hat{x}_{k,i}^{(\text{data})} = y_{\mathcal{D}_k(i)}/h_{k,\mathcal{D}_k(i)} \ , \quad i = 1, 2, \ldots, N_{\text{data}} \ , \qquad (4)$$

where $\mathcal{D}_k$ is the set of indices where the mapping pattern of the kth device is non-zero. In other words, only the symbols from the non-zero positions of the device pattern are read out. The normalized log-likelihood-ratios (LLRs) are then computed and scaled by the corresponding signal-to-interference-plus-noise ratio (SINR) values, which are equal to

$$\text{SINR}_{k,i}^{(\text{data})} = \frac{|h_{k,\mathcal{D}_k(i)}|^2}{\sum_{\substack{l \in \mathcal{L}_k(i) \\ l \neq k}} |h_{l,\mathcal{D}_k(i)}|^2 + \sigma_n^2} \ , \qquad (5)$$

where $\mathcal{L}_k(i)$ is the set of devices with non-zero positions at the $\mathcal{D}_k(i)^{\text{th}}$ symbol index, and σ_n^2 is the noise variance. Afterwards, channel decoding is performed, and the devices that pass the cyclic-redundancy-check (CRC) are removed from the received signal.

III. SIMULATION SCENARIO

A. Setup

We consider a scenario in which multiple vehicles broadcast their messages (e.g., safety-critical messages) to their surroundings, and we evaluate the performance at a vehicle that is receiving those messages. Due to the nature of grant-free NOMA transmission, the receiving vehicle first has to perform user activity detection to figure out which patterns are active, combined with channel estimation [9]. Here, we assume perfect user activity detection and channel estimation, and focus on the potential performance. Since this is a link-level study, we do neither consider a network geometry nor traffic models to reflect on the generated load. Instead, we evaluate the performance over the collision probability. This

6 Parameter	Value
# transmitting vehicles N_v	$1, 2, 3, 4$
Expansion factor L	1.5
# patterns	8
Center frequency	5.9 GHz
Subcarrier spacing	15 kHz
# selected subcarriers	180
Transmission duration	2 slots (14 OFDM symbols)
Average SNR and spread	11 dB, ± 3 dB
Channel model	TDL-C with Jakes spectrum
RMS delay spread	100 ns
Relative velocity	100 km/h
Modulation	4-QAM
OMA code-rate R_b	1/6
NOMA code-rate R_b'	$1/6 \times L$
Channel code	LTE turbo
# max PIC iterations	$I_{\text{outer}} = 5$

TABLE I: Simulation parameters.

allows us to abstract a lot of system-level parameters that would be required to describe a vehicular scenario into a single parameter. Parameters such as vehicle density, the generated traffic, or the collision avoidance algorithm; all of those translate in the end into a specific value of the collision probability. Therefore, by sweeping over the collision probability, we can cover various configurations. Let the collision probability be p_{col}, at every simulation repetition, a value is drawn from a Bernoulli distribution characterized by p_{col}. When 0 is drawn, only one vehicle occupies the resources and the transmission is collision-free. If the drawn value is 1, collision occurs.

The mapping patterns were generated randomly by first constructing a row-vector with exactly N_{data} ones and $N_{\text{total}} - N_{\text{data}}$ zeros; the patterns are then obtained by a random shuffle of this base vector. In practice, those patterns would be generated only once and defined in the standard. One option is to construct a single base pattern randomly, and then the other patterns are generated by a cyclic-shift of this base pattern [18], or via a power method, which also requires a single base pattern [19]. In the end, we obtain a pattern matrix that is similar to (1). The total number of generated patterns are eight, and a transmit vehicle chooses one of the patterns randomly at every simulation repetition. Therefore, it is possible that multiple vehicles pick the same pattern. The channel realizations were generated according to the tapped-delay-line-C (TDL-C) channel model [20] with Jakes Doppler spectrum. The various PHY operations, such as channel coding, modulation, and channel generation are carried out using the Vienna 5G Link-Level Simulator[1] [21]. To produce time-selectivity, the relative velocity of the vehicles is set to 100 km/h. The transmit powers are chosen such that their average signal-to-noise ratios (SNRs) at the receiving vehicle are uniformly distributed in the range $[8, 14]$ dB, that is, 11 dB plus a uniform spread of ± 3 dB. This would correspond to the difference in pathloss between the vehicles. The parameters are summarized in Table I.

Fig. 3: Impact of varying the expansion factor L.

Fig. 4: Performance of the grant-free NOMA scheme vs OMA.
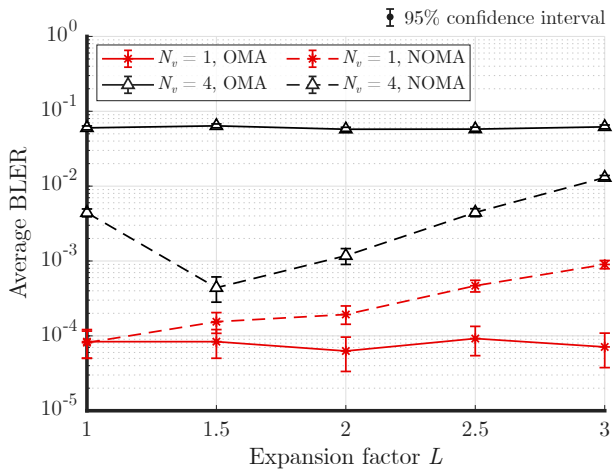
B. Average BLER

First, we investigate the impact of varying the expansion factor L on the average BLER performance at the receiving end. We fix the collision probability to 0.1, and we consider the case of four transmitting vehicles ($N_v = 4$). As a reference, we show the performance of an OMA system that decodes the packets directly without taking any measure to resolve the collisions, and also the performance of a NOMA and OMA single-vehicle transmission ($N_v = 1$), i.e., no collisions. Those are shown in Figure 3. We observe that there is a sweet spot for L. Setting it too high will shift a large amount of redundancy to the symbol-level, which in turn sacrifices the gain of channel coding, since the code-rate is increased as well. On the other hand, setting L to 1 means that no expansion is performed, and the NOMA transmission is identical to OMA. The reason why the NOMA setup at $L = 1$ is performing better than OMA is due to the employment of PIC, which helps in resolving the collisions. For the considered scenario of four transmitting vehicles, it appears that $L = 1.5$ provides a good trade-off between the amount of symbol- and bit-level redundancy, when compared to the baseline of a single-vehicle transmission.

Next, we evaluate performance for a different number of transmitting vehicles at different values of the collision probability p_{col}. This is shown in Figure 4. The NOMA framework is very robust to collisions. For the two vehicles case ($N_v = 2$) and at a high collision probability, we see that the performance loss due to collisions is much smaller compared to the OMA system. For a higher number of colliding vehicles, the loss is larger; however, it is still substantially better than an OMA system that does not resolve collisions. Also, we notice that the performance of OMA does not fall exactly on the line BLER $= p_{col}$, but rather depends on N_v. That is because even when a collision occurs, the receiver still attempts to decode the packets, and therefore some of them might be decoded correctly when N_v is low.

In the low collision probability regime ($< 10^{-2}$), the performance gap gets smaller, suggesting that if such a system
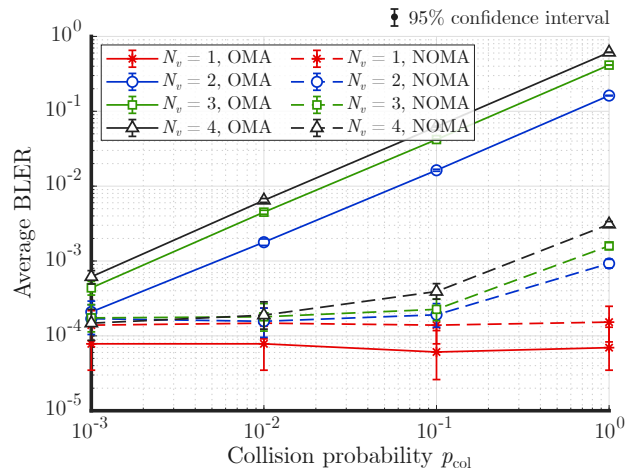
is combined with a highly performing collision avoidance algorithm and a moderate vehicle density, then the benefit of applying grant-free NOMA might be less sound. However, this is also dependent on the BLER performance of the system without collisions. For example, if the collision-free BLER is 10^{-5}, then even a collision probability of 10^{-3} might result in a large gap between OMA and NOMA.

C. Link Outage Duration

To investigate the impact of applying such a scheme in terms of the transmission latency, we evaluate the outage duration of the link. We define the outage as the number of dropped packets between two successfully received packets. If two consecutive packets are received correctly, then the outage is zero. If two packets were dropped in between, then the outage is two, and so on. This is illustrated in Figure 5.
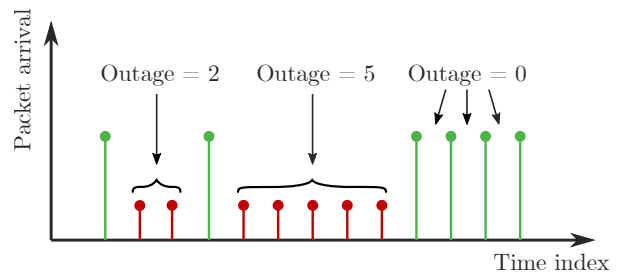

Fig. 5: Illustration of the outage calculation. Green steps represent packets that are successfully decoded, while red steps represent the dropped packets.

We run simulations with the same parameters as in the previous section ($L = 1.5$), and plot the obtained empirical cumulative distribution function (ECDF) of link outage for one of the transmissions. This is shown in Figures 6 and 7, for $N_v = 2$ and 4 vehicles, respectively. The NOMA system sustained low outages even for $p_{col} = 1$. For that reason, we only plot the $p_{col} = 1$ case for NOMA, as the other cases were much lower. Also, for better visualization, the x-axis of the ECDF was truncated to 10 packets.
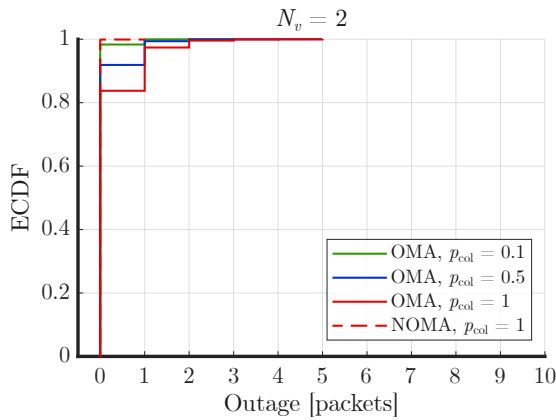
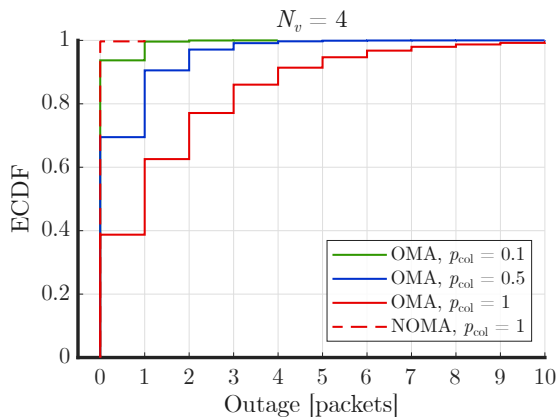Fig. 6: ECDF of the outage duration for $N_v = 2$.

Fig. 7: ECDF of the outage duration for $N_v = 4$.

It can be observed that the OMA system suffers from longer outage durations when a high number of vehicles collide. The NOMA system, on the other hand, is able to sustain extremely low outage durations, even in the case where four vehicles are constantly colliding ($p_{col} = 1$). Of course, this is a distribution tail problem; longer outages might occur if more simulation repetitions are considered, but at least that was the trend for the 10^5 simulation repetitions considered here. Similarly to the BLER results, we see that the gap gets smaller between OMA and NOMA as the collision probably approaches zero.

IV. Conclusion

In this work, we investigate applying the framework of grant-free NOMA to V2X communication when there is no central coordination by the BS. A scheme based on a spread mapping of the data symbols is applied as a candidate scheme and has its performance benchmarked, showing a potential gain in terms of robustness to collisions. The gains were demonstrated in terms of both the average BLER and packets outage duration. The results suggest that the benefit of employing the NOMA scheme compared to OMA is dependent on which operating point the system offers in terms of the collision probability and the collision-free BLER performance.

References

[1] K. Abboud, H. A. Omar, and W. Zhuang, "Interworking of DSRC and Cellular Network Technologies for V2X Communications: A Survey," *IEEE Transactions on Vehicular Technology*, vol. 65, no. 12, pp. 9457–9470, Dec 2016.

[2] S. Schwarz, T. Philosof, and M. Rupp, "Signal Processing Challenges in Cellular-Assisted Vehicular Communications: Efforts and developments within 3GPP LTE and beyond," *IEEE Signal Processing Magazine*, vol. 34, no. 2, pp. 47–59, March 2017.

[3] Z. Amjad, A. Sikora, B. Hilt, and J. Lauffenburger, "Low Latency V2X Applications and Network Requirements: Performance Evaluation," in *2018 IEEE Intelligent Vehicles Symposium (IV)*, June 2018, pp. 220–225.

[4] G. Naik, B. Choudhury, and J. Park, "IEEE 802.11bd 5G NR V2X: Evolution of Radio Access Technologies for V2X Communications," *IEEE Access*, vol. 7, pp. 70 169–70 184, 2019.

[5] V. Mannoni, V. Berg, S. Sesia, and E. Perraud, "A Comparison of the V2X Communication Systems: ITS-G5 and C-V2X," in *2019 IEEE 89th Vehicular Technology Conference (VTC2019-Spring)*, April 2019, pp. 1–5.

[6] M. Gonzalez-Martín, M. Sepulcre, R. Molina-Masegosa, and J. Gozalvez, "Analytical Models of the Performance of C-V2X Mode 4 Vehicular Communications," *IEEE Transactions on Vehicular Technology*, vol. 68, no. 2, pp. 1155–1166, Feb 2019.

[7] Z. Wu, K. Lu, C. Jiang, and X. Shao, "Comprehensive Study and Comparison on 5G NOMA Schemes," *IEEE Access*, vol. 6, pp. 18 511–18 519, 2018.

[8] M. B. Shahab, R. Abbas, M. Shirvanimoghaddam, and S. J. Johnson, "Grant-free Non-orthogonal Multiple Access for IoT: A Survey," 2019.

[9] L. Tian, C. Yan, W. Li, Z. Yuan, W. Cao, and Y. Yuan, "On uplink non-orthogonal multiple access for 5g: opportunities and challenges," *China Communications*, vol. 14, no. 12, pp. 142–152, December 2017.

[10] B. Di, L. Song, Y. Li, and Z. Han, "V2X Meets NOMA: Non-Orthogonal Multiple Access for 5G-Enabled Vehicular Networks," *IEEE Wireless Communications*, vol. 24, no. 6, pp. 14–21, Dec 2017.

[11] S. Hu, B. Yu, C. Qian, Y. Xiao, Q. Xiong, C. Sun, and Y. Gao, "Nonorthogonal Interleave-Grid Multiple Access Scheme for Industrial Internet of Things in 5G Network," *IEEE Transactions on Industrial Informatics*, vol. 14, no. 12, pp. 5436–5446, Dec 2018.

[12] Li Ping, Lihai Liu, Keying Wu, and W. K. Leung, "Interleave division multiple-access," *IEEE Transactions on Wireless Communications*, vol. 5, no. 4, pp. 938–947, April 2006.

[13] H. Nikopour and H. Baligh, "Sparse code multiple access," in *2013 IEEE 24th Annual International Symposium on Personal, Indoor, and Mobile Radio Communications (PIMRC)*, Sep. 2013, pp. 332–336.

[14] Z. Yuan, G. Yu, W. Li, Y. Yuan, X. Wang, and J. Xu, "Multi-User Shared Access for Internet of Things," in *2016 IEEE 83rd Vehicular Technology Conference (VTC Spring)*, May 2016, pp. 1–5.

[15] B. Tahir, S. Schwarz, and M. Rupp, "Constructing Grassmannian Frames by an Iterative Collision-Based Packing," *IEEE Signal Processing Letters*, vol. 26, no. 7, pp. 1056–1060, July 2019.

[16] Y. Cao, H. Sun, J. Soriaga, and T. Ji, "Resource Spread Multiple Access - A Novel Transmission Scheme for 5G Uplink," in *2017 IEEE 86th Vehicular Technology Conference (VTC-Fall)*, Sep. 2017, pp. 1–5.

[17] J. Zhang, Y. Pan, and J. Xu, "Compressive Sensing for Joint User Activity and Data Detection in Grant-Free NOMA," *IEEE Wireless Communications Letters*, vol. 8, no. 3, pp. 857–860, June 2019.

[18] L. Han, M. Jin, and E. Song, "Matrix Cyclic Shifting Based Interleaver Design for IDMA System," in *2009 5th International Conference on Wireless Communications, Networking and Mobile Computing*, Sep. 2009, pp. 1–4.

[19] H. Wu, L. Ping, and A. Perotti, "User-specific chip-level interleaver design for IDMA systems," *Electronics Letters*, vol. 42, no. 4, pp. 233–234, Feb 2006.

[20] 3rd Generation Partnership Project (3GPP), "Technical Specification Group Radio Access Network; Study on channel model for frequency spectrum above 6 GHz," 3rd Generation Partnership Project (3GPP), TR 38.900, Jun. 2018.

[21] S. Pratschner, B. Tahir, L. Marijanovic, M. Mussbah, K. Kirev, R. Nissel, S. Schwarz, and M. Rupp, "Versatile mobile communications simulation: the Vienna 5G Link Level Simulator," *EURASIP Journal on Wireless Communications and Networking*, vol. 2018, no. 1, p. 226, Sep. 2018.